AIAA Paper 89-1945, June 1989.

[7]Tai, C. H., Yin, S. L., and Soong, C. Y., "A Novel Hyperbolic Grid Generation Procedure with Inherent Adaptive Dissipation," *Journal of Computational Physics* (submitted for publication).

[8]McMillin, S. N., Thomas, J. L., and Murman, E. M.,"Navier-Stokes and Euler Solutions for the Lee-Side Flows over Supersonic Delta Wings," NASA TP-3035, Dec. 1990.

[9]Obayashi, S., and Goorjian, P. M., "Improvements and Applications of a Streamwise Upwind Algorithm," AIAA Paper 89-1957, June 1989.

Unstructured Viscous Grid Generation by the Advancing-Layers Method

Shahyar Pirzadeh*
ViGYAN, Inc., Hampton, Virginia 23666

Introduction

DURING the past few years, computational fluid dynamics has progressed to the point that routine, accurate inviscid-flow computations are now possible for practical, realistic configurations in short periods of time. A significant contribution to the recent accomplishment has been due to the emergence of new, efficient grid generation techniques. Unstructured grids, for example, have been extremely successful in simplifying the discretization of complex computational domains for inviscid-flow computations. However, the generation of unstructured grids for routine computation of the Navier-Stokes equations remains a challenging task. Unlike the variety of the Euler grid generation techniques available, there are only a few methods in the literature addressing the problem of viscous, unstructured or hybrid structured/unstructured grid generation. Among these are the methods reported in Refs. 1–4. Relying on the conventional structured grid techniques, some of the existing methods retain the limitations of structured grids and, thus, may lack the required flexibility and robustness for handling complex configurations.

This paper introduces an alternate approach for generating highly stretched unstructured triangular grids. The method is entirely based on an advancing-front technique and, thus, benefits from the flexibility and grid quality of the conventional advancing-front-based Euler grid generators. In this Note, the basic concept of the methodology and some preliminary results in two dimensions are presented.

Approach

The proposed grid generation process is divided into three separate stages: 1) surface grid generation, 2) construction of high-aspect-ratio cells in the viscous-dominated flow region, and 3) generation of a regular (isotropic) grid outside the boundary layer. An existing robust advancing-front-based Euler grid generation system (VGRID)[5,6] is used to perform steps 1 and 3.

Because of the high-aspect-ratio requirement for cells in the boundary layer, a regular advancing-front strategy, like that conventionally used for Euler grid generation, is inadequate for the generation of highly stretched grids without extensive modifications. Such enhancement would require an automatic distribution of grid points densely in one direction and sparsely in other(s) in the boundary layer, and isotropic point distribution elsewhere. This, in turn, would require additional information regarding a variant, multidirectional grid stretching prescribed in the field and a sophisticated mechanism for smooth distribution of stretching data and coordinate transformations. All of these additional elements would adversely affect the entire process of the conventional advancing front for constructing cells of high (several orders of magnitude) aspect ratio and extremely small spacing.

The process of viscous grid generation is greatly simplified if the construction of high-aspect-ratio cells in the boundary layer is performed separately from that of regular unstretched cells outside the viscous-flow region. To that end, a special advancing-front strategy, referred to here as "advancing layers," has been devised for specific generation of stretched cells (step 2). The goal is to maintain the desirable features of the original advancing-front method, i.e., high degree of flexibility, robustness, and good grid quality. The new method is compatible with and supplemental to the conventional advancing-front technique. Although the overall procedure employs two different techniques in separate stages, the entire process is performed continuously with an automatic switch from one method to another.

As in the conventional advancing-front technique, grid cells begin forming individually from the boundaries and march into the domain. However, unlike the generation procedure of the conventional method in which cells are added in no systematic sequence, the construction of a stretched grid is performed by advancing one layer of cells at a time. This strategy is employed to 1) minimize the front congestion, 2) minimize the complexity of search-and-check operations when forming a cell, and 3) evenly distribute stretched cells on all solid boundaries as much as possible. By bringing this order into the advancing-front process, not only does the operation become less complicated, but its efficiency also improves considerably.

Because of the concentration of grid points over a small length scale across the boundary layer, the position of each new point being introduced in the field has a significant effect on the quality of the generated viscous grid. Likewise, the complexity of the grid marching process largely depends on the arrangement of grid points in the boundary layer, especially at sharp corners. To ensure a good grid quality and to facilitate the process, new grid points are positioned along a set of predetermined vectors. The vectors are determined once at each surface mesh point by simply averaging the normal vectors of the faces sharing the point and then smoothing the vectors by a Laplacian smoothing operation. Although this simple procedure is sufficient for calculating the surface vectors in two dimensions, it requires further treatment for three-dimensional problems to prevent the formation of overlapped cells at sharp convex corners.

The advancing-layers process proceeds by successively selecting faces from a list of active faces on the front and connecting them to the new points inserted along the corresponding surface vectors (Fig. 1). The distribution of grid points along the vectors is determined by a stretching function. This is in contrast to prescribing point distribution from information stored in a background grid as is used in the conventional advancing-front method.[7] After a cell is constructed, the old face becomes inactive and is removed from the front, and new faces are created and added to the list. Three types of faces are identified (see Fig. 1) on the front as the layers advance in the field: 1) faces with both nodes on the same layer (level) referred to as primary faces, 2) faces with their nodes on different levels and along different surface vectors (secondary faces), and 3) faces with nodes on different levels but along the same vector (cross-sectional faces). Only the primary and secondary faces are selected to form cells. Although considered active, a cross-sectional face is simply skipped as it will eventually be removed along with an adjacent primary or secondary face. To form

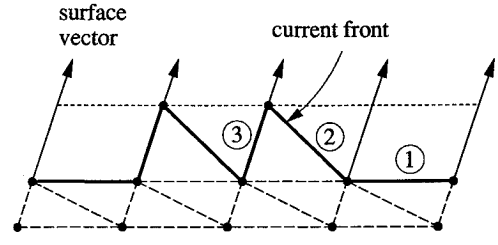

Fig. 1 Layers of triangular cells with different face types on the front: 1) primary face, 2) secondary face, and 3) cross-sectional face.

Received June 8, 1993; presented as Paper 93-3453 at the AIAA 11th Applied Aerodynamics Conference, Monterey, CA, Aug. 9–11, 1993; revision received Feb. 4, 1994; accepted for publication Feb. 7, 1994.

*Senior Research Engineer, 30 Research Drive. Member AIAA.

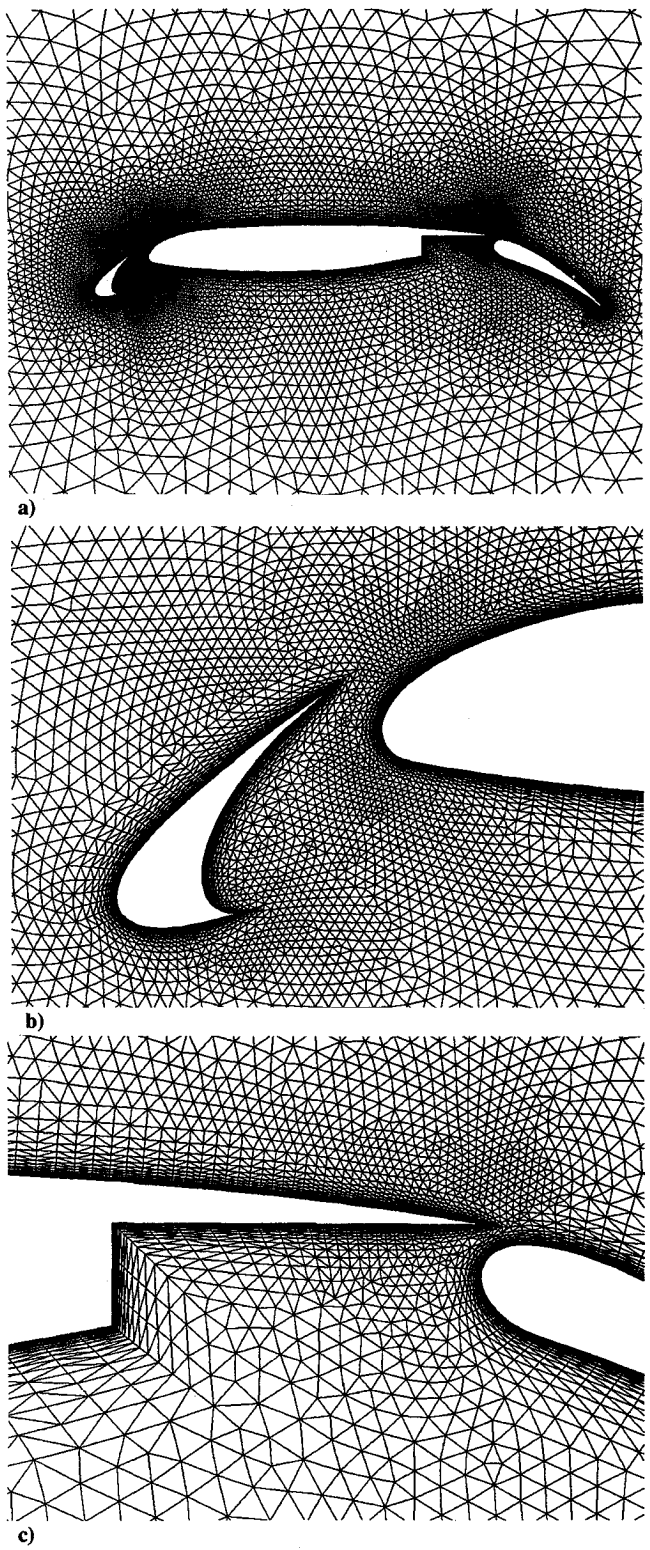

Fig. 2 Unstructured triangular viscous grid around a multielement airfoil: a) complete configuration, b) front section, and c) aft section of main airfoil.

a cell, one or two new ideal points are provisionally considered for the secondary or primary faces, respectively. Layers of cells continue to form and advance in the field in this fashion, while growing in thickness, until certain conditions are locally satisfied on the front. Grid cells stop marching at a location when either two opposing fronts approach or the grid quality, as monitored by a background grid, becomes unacceptable.

To prevent fronts from crossing each other, a search-and-check operation must be performed before a new cell is actually constructed. In addition to the new ideal point(s), all existing close points are identified, and their proximity to the face under consideration is checked. The criterion by which the candidate points are evaluated has a significant impact on the grid quality and the marching process. Because of the high-aspect-ratio requirement of cells in the boundary layer, and because there is no coordinate transformation involved in the present method, the conventional criteria based on the cell angles[5] are not adequate for generation of highly stretched cells. Instead, a new criterion based on a spring analogy is introduced and used in this work. The candidate points, while fixed in space, are assumed to be connected to the end points of the face to be removed by tension springs. Among the candidate points, the one with the smallest spring force is considered the most appropriate to form the next cell. When an existing point other than a new ideal point is selected for a face to be removed, the indication is that an opposing front is very close to that location, and no more layers of cells grow on that face.

Even though a background grid does not directly determine the distribution of grid points during the generation of cell layers (as it does in the conventional advancing-front method), it controls the extent by which the individual layers of cells grow in the field. The advancing process terminates on a face when the local grid characteristics on the front, influenced by the stretching function, no longer match those determined by the background grid in that location. When the proximity and/or grid quality criteria are satisfied on all faces on the front, the process automatically switches from the advancing-layers to the conventional advancing-front grid generation method to form regular isotropic cells in the rest of the domain. The criteria ensure a flexible convergence of approaching fronts and a smooth transition from a viscous, highly stretched grid to an inviscid, regular grid.

Results

A sample, triangular, viscous grid around a complex multielement airfoil is presented to demonstrate the capability of the new approach. The geometry consists of three airfoil sections in a high-lift arrangement. The generated grid, shown in Fig. 2, contains 34,987 cells, 17,705 points, and 427 boundary points with a first-layer spacing of about 7×10^{-6} main airfoil chord lengths. The overall smoothness of the grid around the complete configuration is evident in Fig. 2a. A close-up view of the grid around the front

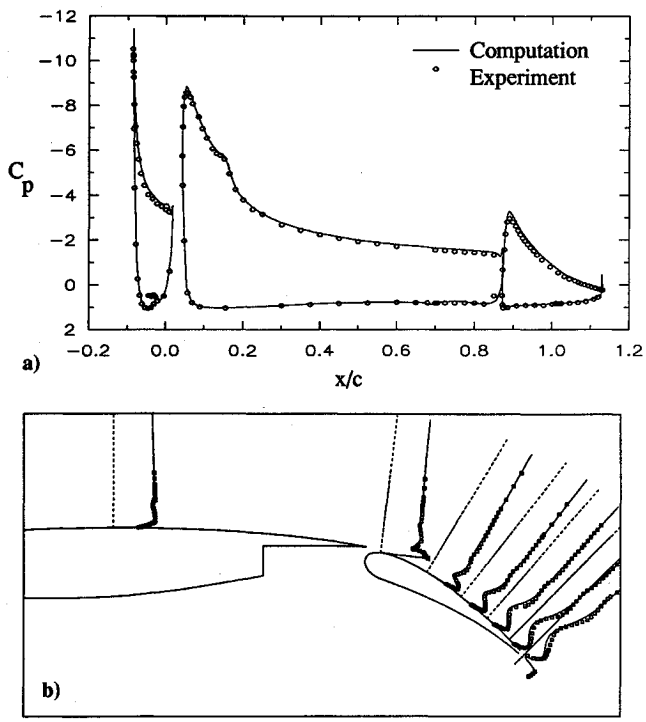

Fig. 3 Viscous-flow computation for a multielement airfoil at M_∞ = 0.2, α = 16.2 deg, and $Re = 9 \times 10^6$: a) surface pressure distributions and b) velocity profiles.

and back portion of the airfoil is shown in Figs. 2b and 2c, respectively. The smooth transition of the grid from one type to another and the decency of the grid at sharp corners and between close surfaces are clearly shown, which indicate excellent compatibility and communication between the two grid strategies as controlled by a common background grid. The grid was generated using a Silicon Graphics IRIS 4D/210 VGX workstation. The code's performance is about 360 triangles/s on that workstation and 2350 triangles/s on a Cray Y-MP. The total turnaround time required for generating a grid around a complex geometry, including the setup time, is about 1 h.

To examine the fidelity of the grids generated with the present method, a turbulent viscous-flow computation was performed on the grid shown in Fig. 2. The flow solution was obtained with an available node-based, upwind flow solver[8] using the Baldwin-Barth turbulence model at a Mach number of 0.2, an angle of attack of 16.2 deg, and a Reynolds number of 9×10^6. Comparisons for surface pressure distributions and velocity profiles are shown in Figs. 3a and 3b, respectively. Excellent agreement with experimental data confirms the viability of the generated grid.

Concluding Remarks

A new method of unstructured viscous grid generation has been introduced. The approach is conceptually simple but powerful, and capable of producing high-quality viscous unstructured grids for complex configurations with ease. Being based on a totally unstructured grid strategy, the method is fully automatic and flexible and, thus, alleviates the difficulties stemming from the structural limitations of the existing structured or semi-unstructured techniques. Because of an efficient grid-marching strategy and a simple front-detection algorithm, the method is highly efficient and operational on small workstations. The method is also self-sufficient for insertion of grid points in the boundary layer and beyond.

The method has been applied to two-dimensional problems with satisfactory results. The basic elements of the technique, however, have been primarily designed for its subsequent extension for generating three-dimensional highly stretched tetrahedral grids which is currently in progress. The full benefit of the method will be realized for generation of three-dimensional viscous grids where the complexity of the problem becomes excessive.

Acknowledgements

This work was sponsored by NASA Langley Research Center, Contract NAS1-19672, with Neal T. Frink serving as technical monitor. The flow result presented in this paper has been provided by Kyle W. Anderson, NASA Langley Research Center, which is gratefully acknowledged.

References

[1]Mavriplis, D. J., "Euler and Navier-Stokes Computations for Two-Dimensional Geometries Using Unstructured Meshes," Inst. for Computer Applications in Science and Engineering, NASA Langley Research Center, Rept. 90-3, NASA CR-181977, Jan. 1990.

[2]Nakahashi, K., "Optimum Spacing Control of the Marching Grid Generation," AIAA Paper 91-0103, Jan. 1991.

[3]Kallinderis, Y., and Ward, S., "Prismatic Grid Generation with an Efficient Algebraic Method for Aircraft Configurations," AIAA Paper 92-2721, June 1992.

[4]Ward, S., and Kallinderis, Y., "Hybrid Prismatic/Tetrahedral Grid Generation for Complex 3-D Geometries," AIAA Paper 93-0669, Jan. 1993.

[5]Parikh, P., Pirzadeh, S., and Löhner, R., "A Package for 3-D Unstructured Grid Generation, Finite Element Flow Solution and Flow Field Visualization," NASA CR-182090, Sept. 1990.

[6]Pirzadeh, S., "Recent Progress in Unstructured Grid Generation," AIAA Paper 92-0445, Jan. 1992.

[7]Pirzadeh, S., "Structured Background Grids for Generation of Unstructured Grids by Advancing Front Method," *AIAA Journal*, Vol. 31, No. 2, 1993, pp. 257–265; also AIAA Paper 91-3233, Sept. 1991.

[8]Anderson, W. K., and Bonhaus, D. L., "An Implicit Upwind Algorithm for Computing Turbulent Flows on Unstructured Grids," *Computers and Fluids*, Vol. 23, No. 1, 1994, pp. 1–21.

Influence of Impingement Edge Geometry on Cavity Flow Oscillations

J. C. F. Pereira* and J. M. M. Sousa†
Instituto Superior Técnico, 1096 Lisbon, Portugal

Introduction

THERE is a variety of engineering flow applications and systems that can be modeled as single or as series of cavities, including slotted-wall wind and water tunnels, aircraft components, depressions in submarine and ship hulls, computer boards with closely spaced chip carriers, or even the gasdynamic laser cavities. Experimentally, it has been observed that the fluid flow in and near cavity-type geometries is unsteady, usually exhibiting large-amplitude oscillations of pressure and velocity. Although it is undeniable that the flow oscillations may be beneficial in certain cases (e.g., to enhance heat transfer rates), in most cases they are pernicious, causing structural vibration and noise, as well as increasing drag. Therefore attenuation of cavity oscillations is a relevant subject.

The experiments of Sarohia[1] for laminar axisymmetric flow have proved that the reported flow oscillations were not a result of resonance phenomena based on the interaction of the separated shear-layer deflection and internal cavity pressures. The mechanism that sustains the oscillations in such impinging flows was later investigated by Rockwell and Knisely.[2] In their work, they have shown that these flows are dominated by vortical structures that form upstream, in the vicinity of the separation edge, and impinge at the downstream edge of the cavity. The presence of this edge leads to an enhancement of the organization of the aforementioned shear layer. Moreover, the interaction between the vortical structures and the impingement corner was found to generate a feedback mechanism, sustaining markedly coherent fluctuations.[3,4] Hence, it is reasonable to expect that modifications of the downstream cavity edge geometry will give rise to important changes in the specific characteristics of cavity flow oscillations. Simple modifications may, from this standpoint, allow for the achievement of a major reduction in the oscillations amplitude.

The present experiments embrace visualization of the shear-layer flow past three different cavity edge geometries (sharp, nose-shape, and round), as well as detailed laser Doppler anemometry measurements of the time-averaged velocity flowfield and turbulent velocity characteristics. The information reported herein aims to characterize the influence of the impingement edge geometry on unsteady cavity flow and it is further used to assess the effectiveness of the modified configurations (nose-shape and round corners) in attenuating the flow oscillations.

Experimental Procedure and Instrumentation

The experimental setup consisted of a cavity model formed on the floor of a water tunnel made of PERSPEX, 0.170 m in depth, 0.200 m in width, and 7 m in length. The water was drawn from a constant-head discharge tank and pumped, in a closed-circuit, into a pressurized tank, as described by Durão et al.[5] The cavity model spanned the test section by a combination of appropriate upstream and downstream plates, yielding a depth-to-cavity length ratio of $h/b = 0.5$ and a depth-to-width ratio of $h/w = 0.12$ for $h/H = 0.141$, where H is the channel height. The incoming turbulent channel flow Reynolds number was $Re_H = 20{,}440$, the turbulence intensity at the channel centerline was approximately 4%, and the corresponding cavity flow was characterized by a Reynolds number, based on the cavity depth h and channel centerline velocity U_O,

Received Jan. 25, 1993; revision received Nov. 30, 1993; accepted for publication Dec. 9, 1993.

*Associate Professor, Department of Mechanical Engineering, Av. Rovisco Pais. Member AIAA.

†Research Assistant, Department of Mechanical Engineering.